Adaptive region of interest method for analytical micro-CT reconstruction

Wanneng Yang, Xiaochun Xu, Kun Bi, Shaoqun Zeng, Qian Liu and Shangbin Chen*
*Britton Chance Center for Biomedical Photonics, Wuhan National Laboratory for
Optoelectronics-Huazhong University of Science and Technology, Wuhan, China*

Abstract. The real-time imaging is important in automatic successive inspection with micro-computerized tomography (micro-CT). Generally, the size of the detector is chosen according to the most probable size of the measured object to acquire all the projection data. Given enough imaging area and imaging resolution of X-ray detector, the detector is larger than specimen projection area, which results in redundant data in the Sinogram. The process of real-time micro-CT is computation-intensive because of the large amounts of source and destination data. The speed of the reconstruction algorithm can't always meet the requirements of real-time applications. A preprocessing method called adaptive region of interest (AROI), which detects the object's boundaries automatically to focus the active Sinogram regions, is introduced into the analytical reconstruction algorithm in this paper. The AROI method reduces the volume of the reconstructing data and thus directly accelerates the reconstruction process. It has been further shown that image quality is not compromised when applying AROI, while the reconstruction speed is increased as the square of the ratio of the sizes of the detector and the specimen slice. In practice, the conch reconstruction experiment indicated that the process is accelerated by 5.2 times with AROI and the imaging quality is not degraded. Therefore, the AROI method improves the speed of analytical micro-CT reconstruction significantly.

Keywords: Adaptive region of interest (AROI), Analytical micro-computerized tomography, Filter backprojection (FBP) algorithm, Feldkamp-type (FDK) algorithm

1. Introduction

The micro-computerized tomography (micro-CT) has become widely used in modern industrial non-destructive testing (NDT), biology and three-dimensional microscopy in recent years [1,2]. With this technique, especially development of flat-panel detector, the interior distribution of density can be acquired without destruction of the object. Specific information about the target, such as magnitude, shape, and measurements, can be obtained intuitively from the 2D or 3D tomography. Real-time micro-CT imaging is important and necessary in automatic successive inspection applications, such as industrial nondestructive testing of small machine components, successive pot-grown plant micro-CT imaging and automatic food inspection. In order to achieve the goal, rapid scanning is one of the key factors

---

*Corresponding author: Shangbin Chen, Britton Chance Center for Biomedical Photonics, Wuhan National Laboratory for Optoelectronics-Huazhong University of Science and Technology, Wuhan 430074, China. Tel.: +86 27 87792033; Fax: +86 27 87792034; E-mail: sbchen@mail.hust.edu.cn.

of real-time imaging. Besides scanning speed, reconstruction speed is another key limiting factor in real-time micro-CT [3–11].

Conventional iterative algorithms take very long computational time because of the iterative projection and backprojection steps. Thus analytical reconstruction algorithms are more suitable for successive real-time micro-CT imaging [12]. The most widely used analytical reconstruction algorithms for fan-beam and cone-beam CT are the filter backprojection (FBP) algorithm and the Feldkamp-type (FDK) algorithm respectively [13–15]. Although these algorithms have been optimized, the reconstruction speed can't yet meet requirements of certain real-time imaging applications. The speed of reconstruction needs to be further accelerated. Pre-weighted, convolution filtering, and backprojection reconstruction are three components of the FBP and FDK algorithms. 98% of reconstruction time is spent on backprojection [13]. Consequently, the most promising approach to accelerate reconstruction is to decrease the processing time for backprojection. Reducing the redundant data and improving the operating speed are the two general ways to decrease the time required for backprojection reconstruction.

In some cases of successive micro-CT imaging system, the size of X-ray detector is often designed larger than that of specimen projection area, which leads to a large amount of redundant data. In some clinical CT or commercial micro-CT systems, the reconstructed region of interest is pre-defined by the operator manually. And in some PET reconstruction, "trimming the Sinogram" is also applied manually to speed up the time-consuming iterative reconstruction [16]. However, in real-time successive imaging for various objects, the method should be adaptive to search the region of interest for different Sinogram.

Benson's FOA algorithm for iterative cone-beam micro-CT reconstruction, which significantly reduced the amount of memory and reconstruction time-consumption, was introduced in 2006 [17]. However, the preprocessing technique of FOA contains one step of backprojecting all projections, which is time-consuming relative to the whole processing of analytical CT reconstruction [12]. Based on this point, it is necessary to develop an adaptive and rapid ROI method for analytical micro-CT reconstruction. This article presents an adaptive region of interest (AROI) method of reducing the image volume for analytical micro-CT reconstruction in the preprocessing phase of the original FBP and FDK.

2. Principles and methods

Generally, in successive real-time micro-CT imaging, the size of the detector is designed and chosen according to the most probable size of the measured object to gather all the projection data. However, the measured object is usually much smaller than the limit size of the system. As a result, the detector will gather much useless data, which increases the reconstruction time without contributing to the result. In order to speed up reconstruction under the condition of enough resolution, this research intended to develop an AROI method to reconstruct only active Sinogram regions automatically. Then only the ROI data will be reconstructed, resulting in reduction of data volume and decrease of processing time (shown in Fig. 1).

Take the general fan-beam projection with the FBP reconstruction algorithm as an example. The number of rotation angles is L, and the number of the linear array X-ray detector elements is N. For simplicity, the rotation center is coincident with the middle of detector elements, so the square size of FOV (field of view) is N^2 (shown as Fig. 1). However, the number of available detector elements is M, so the actual reconstructed area is a square with $M \times M$ pixels, which means that only M^2 of the total N^2 data points are useful in the reconstructed image. The main implementations of the FBP method is based on pixel driven backprojection operator whose time-consumption of each pixel is uniform. So, if the M^2 pixels of the measured object are reconstructed rather than the N^2 pixels, the reconstruction
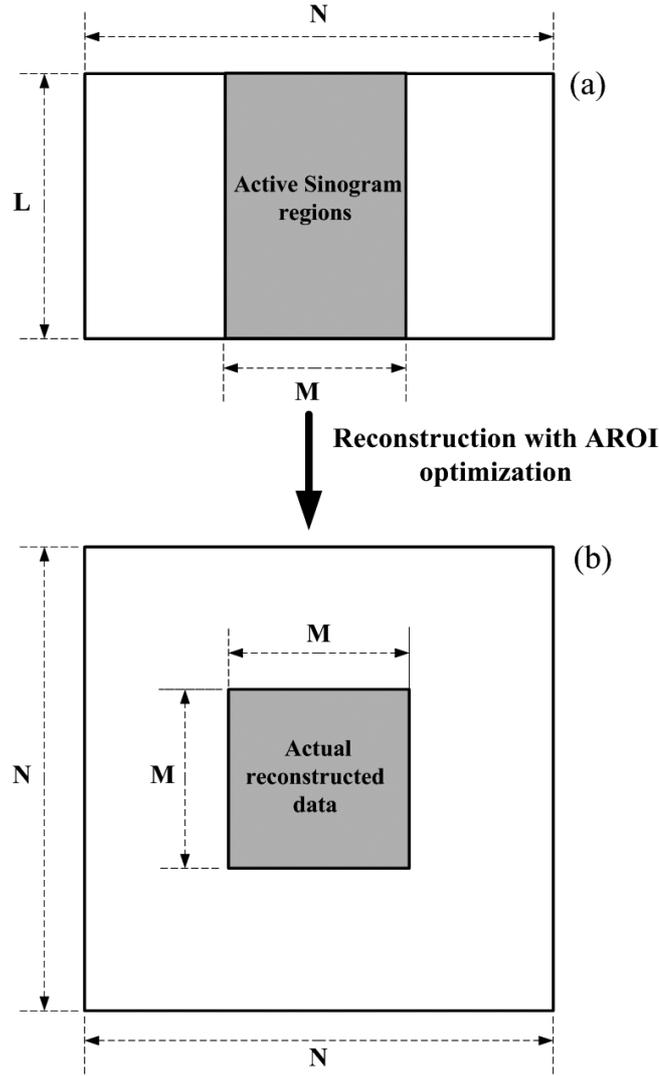
Fig. 1. Schematic diagram of FBP reconstruction algorithm with the AROI method: (a) the scale of Sinogram; (b) the scale of reconstructed image; N is the number of the linear array X-ray detector elements; L is the number of rotation angles; and M is the number of available detector elements with the AROI method.

speed can be accelerated by $(N/M)^2$ times for the parallel-beam or fan-beam FBP algorithm. The speed ratio is time consumption with the original method divided by the time consumption with the AROI method. The width ratio is the detector width divided by the projection object width, as for N/M above. Therefore, the relationship between the speed ratio and the width ratio is:

$$y = x^2 \tag{1}$$

Where x is the width ratio and y is the speed ratio. Moreover, the AROI method affects only the background of the reconstruction image, and the reconstruction quality of the specimen will not be degraded.

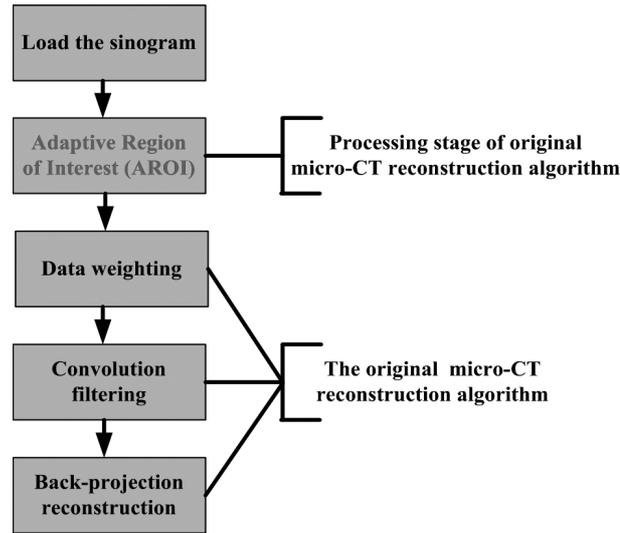The flowchart of the micro-CT reconstruction algorithm (FBP and FDK algorithm) with AROI opti-

Fig. 2. Flowchart of micro-CT reconstruction algorithm with the AROI method.
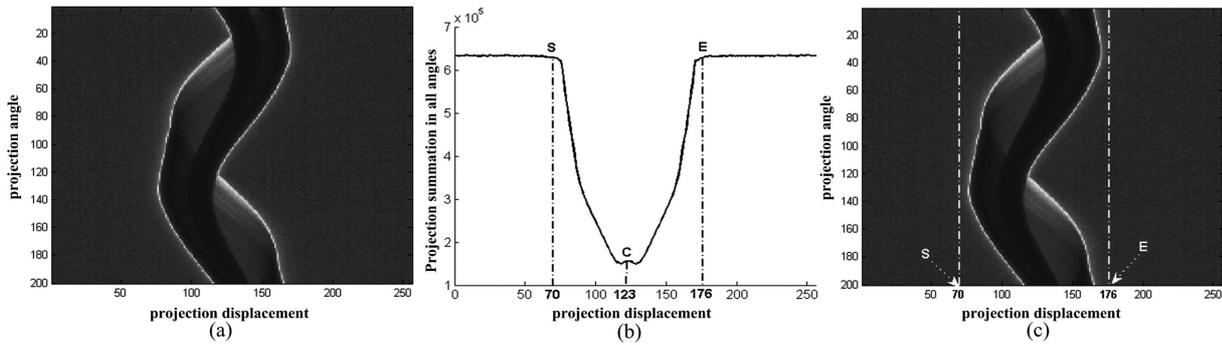

Fig. 3. Steps of AROI: (a) conch slice projection data with a cone-beam micro-CT; (b) dimension reduction for searching S point and E point; (c) the edge of the actual object data as shown by white dashed lines.

mization is shown in Fig. 2. The original FBP and FDK reconstruction algorithms include three steps: data weighting, convolution filtering, and backprojection reconstruction. A new 3D FOA approach for iterative micro-CT reconstruction was developed to identify a three-dimensional region of interest automatically by Benson and Gregor in 2006 [17]. However, the FOA algorithm as a data-driven preprocessing technique, including one step of backprojecting all projections, is time-consuming relative to analytical micro-CT reconstruction. Before the first step of the original reconstruction, we directly use the object's boundaries as detected in the Sinogram to focus the active regions without backprojecting.

In order to find the region of interest, the start displacement (shown as S point in the Fig. 3(c)) should first be calculated in the Sinogram, and the end displacement (shown as E point in the Fig. 3(c)) can be certain according to the rotation center of system. For instance, if the rotation center is C, then E can be calculated with the following constraint: $S + E = 2C$. Finally, the boundary of the Sinogram can be easily determined as the interval area between both white dashed lines (shown in the Fig. 3(c)).

The crucial problem in the AROI method is how to automatically identify the start displacement in Sinogram. We find a solution with degrading dimension, converting 2D data of Sinogram to 1D data.
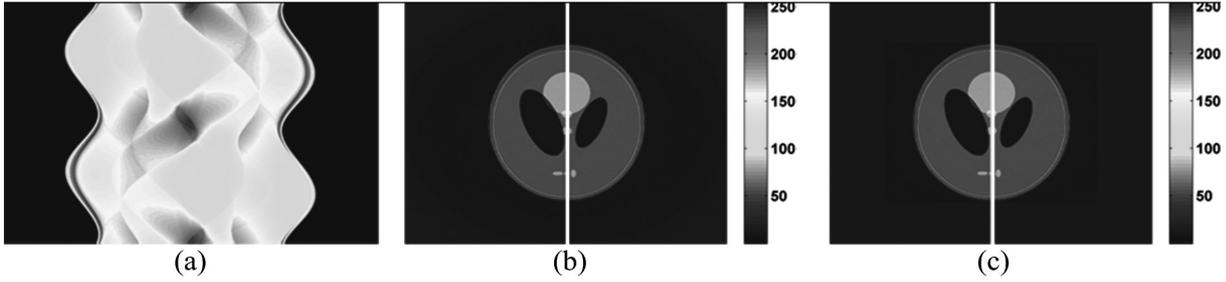
Fig. 4. Shepp-Logan model reconstruction: (a) projection data of the Shepp-Logan model; (b) reconstruction image without AROI optimization; (c) reconstruction image with AROI optimization.

For each displacement, projection summation in all angles constructed a curve shown in Fig. 3(b). On condition that the detector is larger than specimen, some external detector elements, far away from rotation center, can't detect any X-ray absorption of the specimen in each projection angle, vice versa. It's the reason why the curve of projection summation declines dramatically on S point, which can be searched as the inflexion on the left of rotation center in the Fig. 3(b). The AROI method is actually the preprocessing step of the original micro-CT reconstruction algorithm, as shown in Fig. 2. Besides the FBP or FDK, this method can be combined with other CT methods such as that proposed by Fu et al. [7].

3. Experiments

Three experiments were performed to analyze the reconstruction quality and reconstruction speed. For the experiments, simulated data, model data and practical data were used. The combination of the FDK and Fu's reconstruction-speed optimization method, referred to as "the original method" below, was chosen to compare with the AROI method in this research [7].

First, both reconstruction quality and reconstruction speed were compared between the AROI method and the original method using simulated data from the Shepp-Logan model [18]. The major parameters of the simulated experiment were described as follows: the size of the projection data set in this model was 1200×731 pixels; the distance between the X-ray source and the detector was 800 pixels; the angle step was $0.3°$; the scan range was $0°$–$360°$.

Then the relationship between the reconstruction speed and the width of the active regions was investigated through construction of a conical plastic sample with a progressively increasing slice width. The major parameters of this model experiment were described as follows: the size of the conical projection was $122 \times 256 \times 200$ pixels; the distance between the X-ray source and the detector was 7425 pixels; the angle step was $1.8°$; the scan range was $0°$–$360°$.

Finally, a practical data set from a conch was constructed to compare the image quality and computation speed. The major parameters of the practical experiment were described as follows: the size of the projection data set in this model was $512 \times 256 \times 200$ pixels; the distance between the X-ray source and the detector was 11917 pixels; the angle step was $1.8°$; the scan range was $0°$–$360°$.

A HP XW6400 computer workstation with a 2.00-GHz (8-CPU) Intel Xeon processor and 3.0 GB of main memory was used to perform the experiments described here. The original and optimized procedures were both programmed in MATLAB, version 7.6.0.324 (The MathWorks Inc., USA).
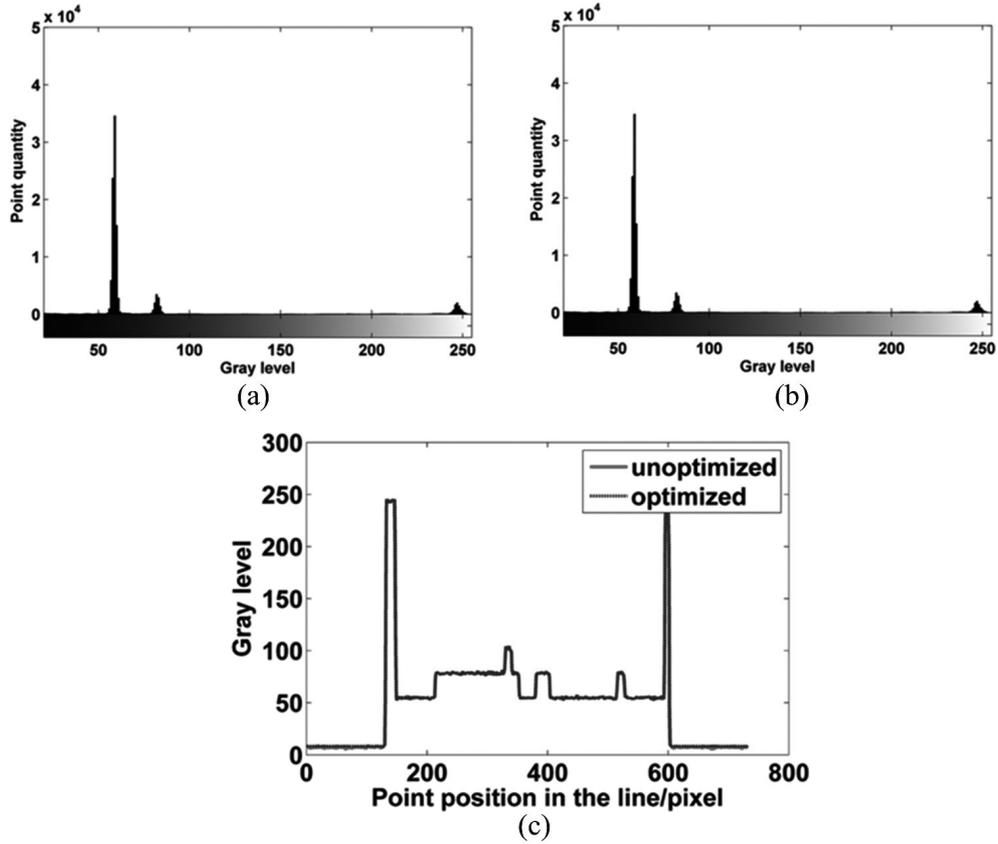
Fig. 5. Comparison of the reconstruction quality of two methods using the Shepp-Logan model. (a) Gray histogram of Fig. 4(b); (b) gray histogram of Fig. 4(c); (c) gray-scale distribution curve of the white lines in Fig. 4(a) and Fig. 4(b). The gray levels in Fig. 5(a) and Fig. 5(b) range from 20 to 255.

4. Results and discussion

4.1. Simulation experiment

A Shepp-Logan model was used to compare both quality and speed of the reconstructed images with the AROI method and the original method. The size of the reconstructed result was 731×731 pixels and time consumption of reconstruction was 88.61 seconds with original method. However, time consumption of reconstruction decreased to 36.03 seconds with the AROI method. Therefore, the reconstruction time was generally decreased to one-third based on the FBP.

A comparison of the reconstruction results is shown in Figs 4 and 5. Figure 5 shows the quality of reconstruction represented by Fig. 4(b) and Fig. 4(c). With the original method, the background gray value of the reconstructed image was less than 20. However, the background gray value of the reconstructed image from the AROI method was 8, as can be seen in Fig. 5(c). The histogram of gray levels from 20 to 255 was chosen to compare the reconstruction quality in Fig. 5(a) and Fig. 5(b). It is clear from the histograms that reconstruction quality of two methods is very similar except the background.
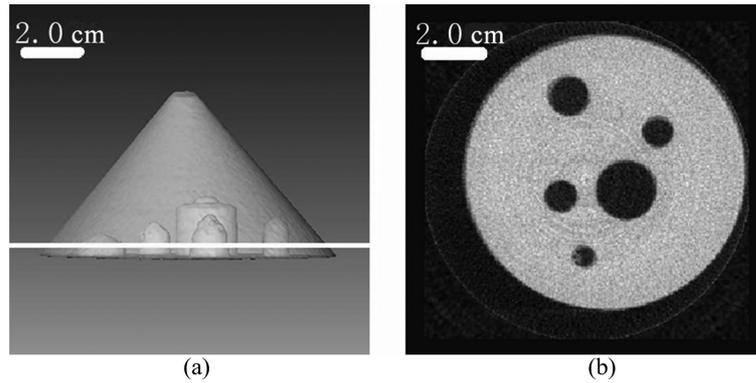
Fig. 6. The conical model reconstruction: (a) 3D reconstruction of the cone; (b) a slice reconstruction image of the white line in Fig. 6(a).
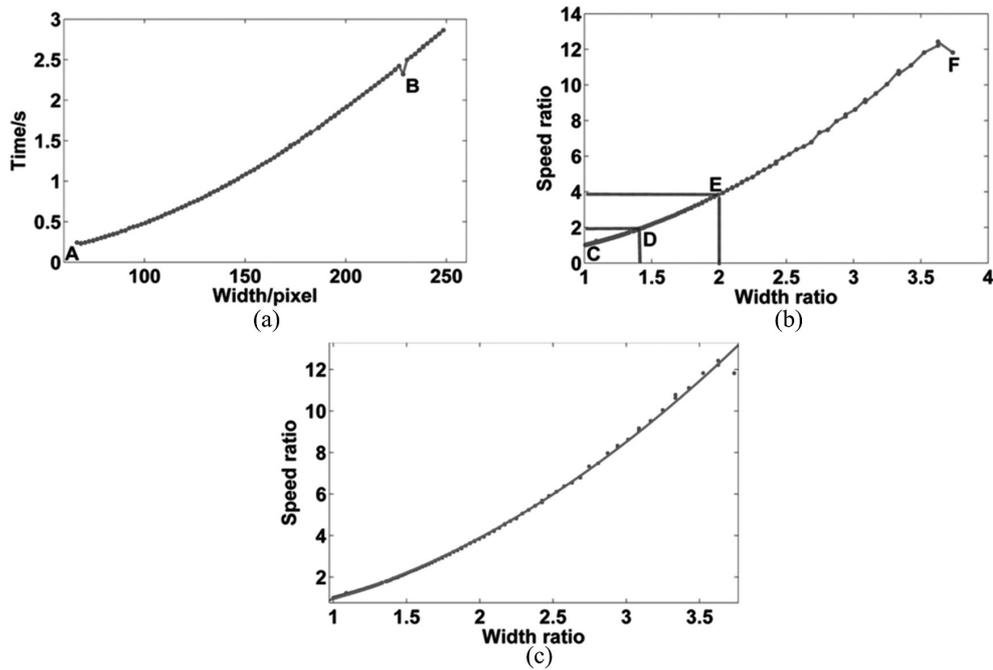

Fig. 7. Reconstruction speed. (a) Relationship between the reconstruction time and the width of the projection image with the AROI method; (b) relationship between the speed ratio and the width ratio of the projection image; (c) curve fitting of the relationship between speed ratio and width ratio. The speed ratio is the time required by the original method divided by the time required by the AROI method. Similarly, the width ratio is the detector width divided by the ROI width.

4.2. Model experiment

A conical plastic sample was manufactured to confirm the relationship between reconstruction speed and the amount of data in a slice. Moreover, to test the relationship between the speed and the internal structure of the object, the conical sample was perforated with five holes with different diameters and depths. The conical sample is shown in Fig. 6. The size of the reconstruction data set was $122 \times 271 \times 271$ pixels.
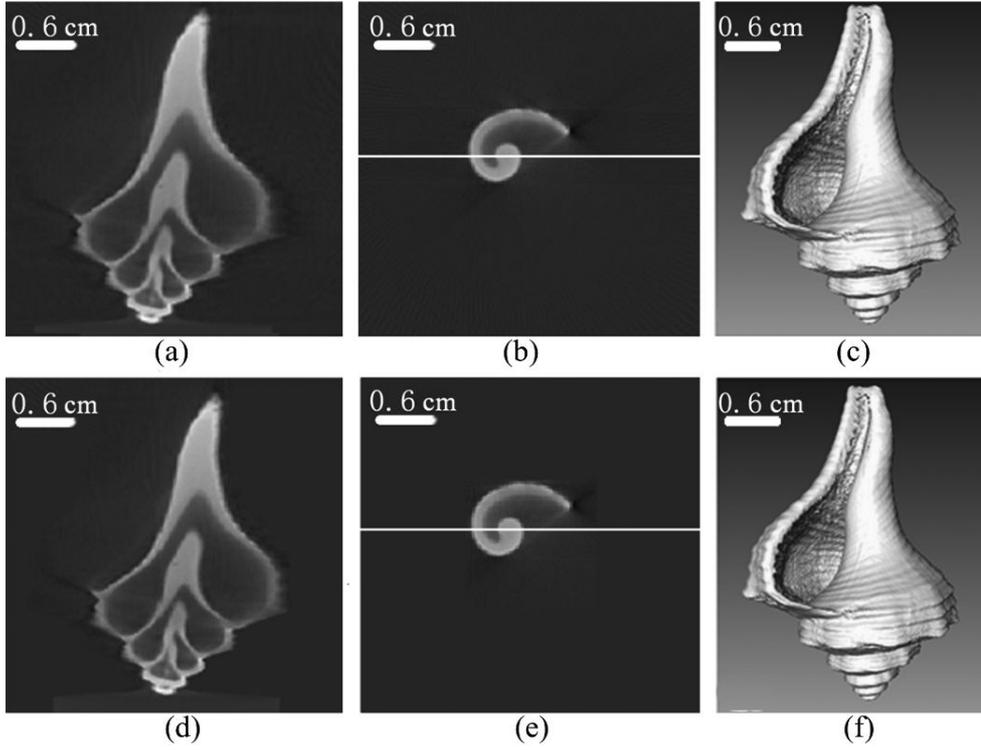
Fig. 8. Reconstruction image of the conch sample. (a), (b), and (c) are the reconstruction images without the AROI method. (d), (e), and (f) are the optimized reconstruction images with the AROI method. (a) and (d) are slice reconstruction images of the y-z plane; (b) and (e) are slice reconstruction images of the x-y plane; (c) and (f) are the 3D reconstruction images.

The relationship between reconstruction speed and the amount of data is shown in Fig. 7. The special point A in Fig. 7 was the first-slice computing time for the reconstruction using the AROI method. This time was slightly longer than for subsequent slices because the computer must first load the reconstruction algorithm code into memory. The operation of loading the algorithm code into memory executed only once from the first time it was called until the end of the application. At point B in Fig. 7, the algorithm spent less time than for the previous point because this point was located in the center slice, whose vertical-direction coordinate in the physical coordinate system was 0. This means that no sine or cosine operator will be executed, and therefore the computing time is slightly shorter than for adjacent slices. When the width of ROI was the same as the detector width, as at point C, the speed of the AROI method was similar to that of the original method. However, at point D, where the width ratio was approximately 1.3, the speed of the AROI method reached twice that of the original method. That is to say, when the width of ROI was 80% of the detector width, the reconstruction speed reached nearly twice that of the original method. Even when the width of ROI was only half the detector width, as at point E, the reconstruction speed reached nearly four times of the original method. Figure 7(c) shows the curve fitted to these data and described by the following equation:

$$y = 0.8811x^2 + 0.2427x - 0.1420 \qquad (2)$$

From the Eq. (2), it can be inferred that the relationship between the speed ratio and width ratio is quadratic, which could be used for predicating reconstruction speed with AROI optimization method.
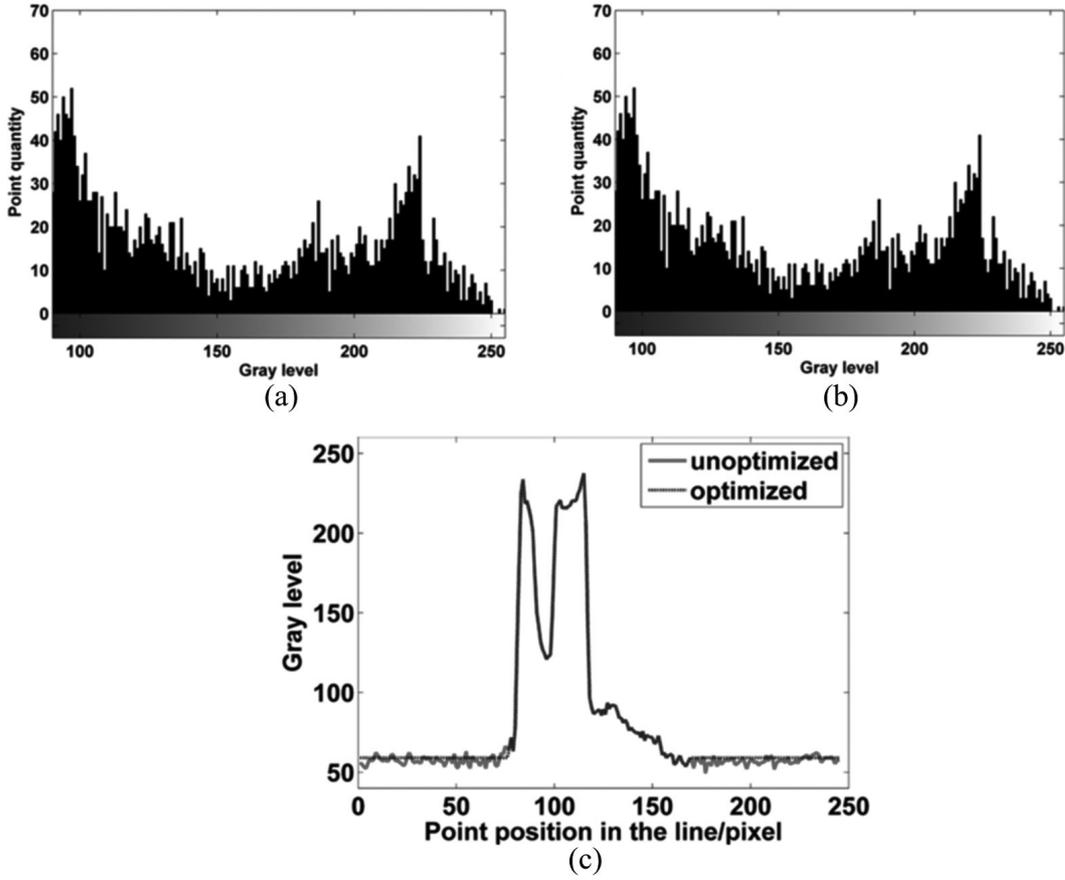
Fig. 9. Comparison of the reconstruction quality of the conch with the two methods. (a) Gray histogram of Fig. 8(b); (b) gray histogram of Fig. 8(e); (c) gray-scale distribution curves of the white lines of Fig. 8(b) and Fig. 8(e), including unoptimized result (deep color) and optimized result (pale color). The gray levels in (a) and (b) range from 90 to 255.

The coefficient of the quadratic term is much larger than the other two coefficients. The coefficient of the first-degree term is not zero because the programs used computed all the data using weighting and filtering. The coefficient of the constant term is close to zero, which may be related to the memory management or compilation methods of MATLAB. Conclusively, the result of the curve fitting is in good agreement with the theoretical analytical results described in Eq. (1). Besides, we should emphasize that the speed ratio does not go exactly as the square of the width ratio due to processor overhead and algorithm behavior, which is specific to the particular implementation and hardware used for the research.

From Fig. 7, it is apparent that the slices with holes also lie on the quadratic curve. Therefore, it can be concluded that reconstruction speed is not influenced by the internal structure of the object when using the AROI method.

4.3. Practical experiment

A conch had been reconstructed from the same projection data using both the AROI method and the original method, as shown in Fig. 8. A slice of the projection data acquired by a cone-beam micro-CT system is shown earlier in Fig. 3(a). The size of the reconstruction data set was $512 \times 245 \times 245$ pixels.

The reconstruction took 1450 seconds overall with the original method. However, only 279 seconds were needed with the AROI method. Therefore, the speed was improved by a factor of approximately 5.2 overall.

Figure 9 shows a comparison of reconstruction quality between Fig. 8(b) and Fig. 8(e). The gray-level histogram values from 90 to 255 were chosen in Fig. 9(c) and Fig. 9(d) because the gray level of the points form the background was less than 90. The gray-level range of the background can be obtained from Fig. 9(c). Figure 9(a) and Fig. 9(b) show that the histograms of the two reconstruction images from the two methods are quite similar except the background.

5. Conclusion

The AROI method, developed for automatic identification of the active Sinogram regions, substantially improves the speed of analytical micro-CT reconstruction. There is a certain relationship between the width of ROI and the reconstruction speed. Compared with the size of the detector, the smaller the measured object, the more significantly the speed improves. In successive real-time micro-CT imaging, the size of the detector is commonly larger than the measured object to meet various measurement demands. When the width of ROI was 80% of that of the detector, the reconstruction speed reached nearly twice that of the original method, and if the width of ROI was only half the detector width, the reconstruction speed reached four times that of the original method. Moreover, the AROI method influences only the background of the reconstruction image, and the reconstruction quality of specimen is not degraded at all. Therefore, AROI is an efficient method for speed optimization of analytical micro-CT reconstruction.

References

[1] T.M. Buzug, *Computed Tomography: from Photon Statistics to Modern Cone-Beam CT*, Springer, Verlag Berlin Heidelberg, 2007.

[2] H. Li, H. Zhang, Z. Tang and G. Hu, Micro-computed tomography for small animal imaging: Technological details, *Progress in Natural Science* **18** (2008), 513–521.

[3] C. Mora, M.J. Rodriguez-Alvarez and J.V. Romero, New pixellation scheme for CT algebraic reconstruction to exploit matrix symmetries, *Computers & Mathematics with Applications* **56** (2008), 715–726.

[4] N. Neophytou, F.X. and K. Mueller, Hardware acceleration vs. algorithmic acceleration: can GPU-based processing beat complexity optimization for CT? *Progress in biomedical optics and imaging* **8**(3) (2007), 65105F.1–65105F.9.

[5] G.C. Sharp, N. Kandasamy, H. Singh and M. Folkert, GPU-based streaming architectures for fast cone-beam CT image reconstruction and demon-deformable registration, *Physics in Medicine and Biology* **52** (2007), 5771–5783.

[6] J. Hsieh, *Computed Tomography: Principles, Design, Artifacts, and Recent Advances*, SPIE Press, Washington, 2003.

[7] J. Fu, H. Lu and Q. Zhang, Speed optimization of reconstruction algorithm for fan beam industrial CT, *CT Theory and Applications* (*Chinese Core Journal*) **11**(3) (2002), 16–19.

[8] K. Bi, Q. Liu, X. lv, Q. Luo and S. Zeng, A LabVIEW driver for X-ray flat–panel detector, *Journal of X-Ray Science and Technology* **16** (2008), 261–268.

[9] P. Danielsson and M. Ingerhed, Backprojection in O(N^{2}logN) time, *IEEE Nuclear Science Symposium* **2** (1997), 1279–1283.

[10] C. Axelsson and P. Danielsson, Three-dimensional reconstruction from cone-beam data in O(N^{3}logN) time, *Physics in Medicine and Biology* **39** (1994), 477–491.

[11] B. Liu and L. Zeng, Parallel SART algorithm of linear scan cone-beam CT for fixed pipeline, *Journal of X-Ray Science and Technology* **17** (2009), 221–232.

[12] B. Lee, H. Lee and Y.G. Shin, Fast hybrid CPU- and GPU-based CT reconstruction algorithm using air skipping technique, *Journal of X-Ray Science and Technology* **18** (2010), 221–234.

[13] A.C. Kak. and M. Slaney, *Principles of Computerized Tomographic Imaging*, IEEE Press, New York, 1988.

[14] G.T. Herman, *Image Reconstruction from Projection: The Fundamentals of Computerized Tomography*, Academic Press, New York, 1980.

[15] L.A. Feldkamp, L.C. Davis and J.W. Kress, Practical cone-beam algorithm, *Journal of the Optical Society of America A* **1** (1984), 612–619.

[16] X. Liu, M. Defrise, C. Michel, M. Sibomana, C. Comtat, P. Kinahan and D. Townsend, Exact rebinning methods for three-dimensional PET, *IEEE Trans Med Imaging* **18** (1999), 657–664.

[17] T. Benson and J. Gregor, Three-dimensional focus of attention for iterative cone-beam micro-CT reconstruction, *Physics in Medicine and Biology* **51** (2006), 4533–4546.

[18] L.A. Shepp and B.F. Logan, Reconstruction of interior head tissue from X-ray transmissions, *IEEE Trans Nuclear Science* **21** (1974), 228–236.